UCRL 15419-2

[redacted]

[redacted]

EG&G
ENERGY MEASUREMENTS

CLIMAX SPENT FUEL DOSIMETRY

PROGRESS REPORT

SEPTEMBER 1982 — JANUARY 1984

JUNE 1984

SANTA BARBARA OPERATIONS
130 ROBIN HILL RD., GOLETA, CALIF. 93117

[redacted]

DISCLAIMER

This work is being conducted under the technical direction of the Lawrence Livermore National Laboratory (LLNL) as part of the Nevada Nuclear Waste Storage Investigations (NNWSI) for the U.S. Department of Energy (DOE).

EG&G
ENERGY MEASUREMENTS

UCRL--15419-2

DE85 001055

CLIMAX SPENT FUEL DOSIMETRY

PROGRESS REPORT

SEPTEMBER 1982 — JANUARY 1984

by

W. Quam and T. DeVore

JUNE 1984

This report is unclassified: Richard E. Tyson
Classification Officer

Work performed for
the Lawrence Livermore National Laboratory under SANL 309-025

SANTA BARBARA OPERATIONS
130 ROBIN HILL RD., GOLETA, CALIF. 93117

CONTENTS

ILLUSTRATIONS

TABLES

1. INTRODUCTION

This report covers work done during FY83. These tasks included: 1) recovery and readout of the final set of dosimeters from the Climax facility, 2) a calibration exposure at the Sandia Gamma Irradiation Facility (GIF) to verify temperature effects during irradiation, and 3) a recalculation of new and existing calibration data over the range of 2×10^3 to 10^8 rads-LiF. This new set of calibration data is slightly different from that previously reported, and incorporates the best temperature corrections determined thus far. Data previously reported[1,2,3] have been corrected and tables of a consistent set of these data are provided.

The high-range dosimetry required for this project was achieved by exploiting the radiation-induced increases in optical absorption in LiF. This phenomenon is manifested as a series of peaks in the absorption spectrum; two of these peaks have proved useful for the dosimetric purposes at hand. The first, centered at 247 nm, covers the range of 2×10^3 to 9×10^6 rads-LiF; while the second, at 374 nm, covers the overlapping range of 2×10^6 to 10^8 rads-LiF. Optical absorption was measured with a double-beam spectrometer in absorbance units (AU), equivalent to the common log of the reciprocal of the optical transmission.

A second short-term (1-h) exposure was done during March 1983, using CaF_2 thermoluminescent dosimeters (TLD's). These data are given in a separate report.[4]

This is the fourth and final report on the LiF dosimetry at the Climax test facility.

2. GAMMA RAY CALIBRATIONS AT ELEVATED TEMPERATURES

The previous report in this series,[3] EG&G Report No. EGG 1183-2455, discussed problems generated by changes in apparent sensitivity when the LiF dosimeters were exposed while at elevated temperatures (60°C to 70°C). Most of the changes seen under these conditions were resolved, but the calibration curve did not extend beyond 2×10^7 rads-LiF at elevated temperatures. Moreover, there appeared to be a slope difference between older data extending to 10^8 rads-LiF (at a nominal 25°C-30°C irradiation temperature) and the newer 60°C data. This slope difference prevented pooling the data into only one set, and the unknown (at the time) temperature coefficient did not allow any corrections to be made for the lower irradiation temperature. Another calibration at a nominal 60°C covering a higher exposure range and some means of correcting for temperatures during irradiation were obviously needed.

We performed several calibration exposures at the EG&G/EM Santa Barbara Operations source range at various temperatures near 60°C and at exposures up to 10^7 rads-LiF. Multiple dosimeters were used and repeated bakeout cycles avoided by adding exposures sequentially. One additional set of exposures was done at Sandia at several temperatures. We also remeasured the exposure rate at Sandia with NBS traceable ion chambers. Because of a different procedure used this time for the Sandia exposures, we were able to retrieve the nominal 25-30°C set very soon after termination of the exposure. It was obvious that there was significant gamma-caused heating of the dosimeter holder used. This made it clear that some of our supposed room-temperature exposures were actually at an elevated temperature (when done at Sandia), and a few comparisons between old data and newer 60°C data showed reasonable agreement if only a small temperature difference was actually present.

We therefore calculated gamma heating effects for all Sandia exposures, taking into account the various dosimeter holder materials used, the room air temperature, and source temperature (since it surrounded the dosimeters during exposure). This resulted in an estimate of 58°C for the stainless steel holder and 53°C for the aluminum holder for exposures greater than 10^7 rads-LiF. The temperature-controlled holders were of course at their nominal set-point since a thermocouple was used to sense the actual holder temperature.

Data taken at Santa Barbara (at a much lower exposure rate and thus insignificant gamma heating) permitted a temperature coefficient at 10^7 rads-LiF near 60°C to be determined. This was $(-0.936 \pm 0.007)\%$ per °C; i.e., as the dosimeter temperature was raised above 60°C, each degree increase resulted in a decrease in apparent AU of 0.936%. This figure together with the calculated dosimeter temperatures from various Sandia irradiations allowed us to determine the 374-nm peak sensitivity at 10^7 rads-LiF at 60°C. If all available data near 10^7 rads-LiF in either stainless steel or aluminum holders from either Santa Barbara or Sandia irradiations are averaged together after correction to 60°C, we find a peak sensitivity of $(0.135 \pm 0.006) \times 10^{-7}$ AU per rad-LiF for six points from seven separate calibration exposures between March 1980 and August 1983.

One exposure in January 1983 was not included in this comparison since it seemed to have obvious problems. It appears that the corrections determined are sufficient to produce calibration data to ±10% at 1 sigma. Furthermore, the calculated LiF exposure temperatures at Sandia are reasonably accurate since the corrected data were part of the average and did not appreciably differ from it. We concluded that all available 374 nm calibration data near 60°C – when suitably corrected for temperature during irradiation – could be pooled together for a common calibration curve.

The LiF chips used as the detectors were "thick" compared to the range of electrons generated by either the ^{60}Co calibration gammas or by the approximately 0.5-MeV gammas encountered in the field exposure. The Appendix illustrates the way in which the data have been handled for both the calibration situation (which resulted in the calibration curves in the next section) and the field measurements.

3. TEMPERATURE-CORRECTED 374 nm CALIBRATION DATA

Some details were provided about the determination of a temperature coefficient for the 374-nm peak. The present section contains calibration data obtained from two different sources corrected to a common 60°C temperature. These data have the following common characteristics:

1. Only data originally at 60 ± 10°C were used. Corrections were made to 60°C because this temperature is near the midpoint of the Climax temperatures. It has no other significance in this report.
2. The 18 points presented were obtained from six separate exposures on two different sources over a 3½-year period. All data are based upon reexamination of the original spectrophotometer records.
3. In 15 of the 18 points, multiple dosimeters were used (10 dosimeters per point in six cases).
4. Dosimeters were exposed in aluminum holders (12 cases) or stainless steel (six cases). Analysis of other data not presented here has shown that irradiations in aluminum and stainless steel may be compared to one another within ±4% at 1 sigma after correcting for absorption of the holder material (see Appendix).
5. Data from exposures at the Sandia GIF were corrected for gamma heating of the holder material if the holder was not remotely heated.

Table 1 presents these data, with columns for various characteristics as noted above. (In the Source column, RS2 is a Santa Barbara Operations ^{60}Co source array, and GIF is the Sandia ^{60}Co source array.)

This same set of data is plotted in Figure 1. A weighted least squares fit yielded the following equation:

$$AU = A\ (\text{exposure})^{B}$$

where

$$A = (1.015 \pm 0.034) \times 10^{-8}$$

$$B = 1.027 \pm 0.0381$$

and the errors are at 95% confidence limits.

The correlation coefficient was 0.9723. A line corresponding to this equation, plotted in Figure 1, was used to determine all new exposure data reported here after the measured AU were corrected to 60°C.

Comparison of this new calibration curve with the previous one (in EG&G Report No. EGG 1183-2455) shows a significant slope change, with a crossover near 2×10^7 rads-LiF. This position of the crossover point has the effect of minimizing differences between old and new data at the wall position, since these exposures are near 2×10^7 rads-LiF. Data from the 0.51-m position as determined from the 374-nm peak show a more pronounced variation between newly corrected and old data. Fortunately the 247-nm peak provides better data in this region (see next section).

Table 1. 374-nm calibration data at 60°C (compiled from data near 60°C originally; see text)

Rads-LiF Exposure	Holder Material	^{60}Co Source	Exposure Date	Beckman 5270 AU ±1 Sigma	Dosimeters per Point
1.55(6)	Aℓ	RS2*	Jun 82	0.018 ±0.002	10
2.55(6)	Aℓ	RS2	Apr 82	0.045 ±0.011	2
3.87(6)	Aℓ	RS2	2 Jun 83	0.065 ±0.008	9
3.87(6)	Aℓ	RS2	Jun 82	0.052 ±0.003	10
5.90(6)	Aℓ	RS2	6 Jun 83	0.088 ±0.008	10
6.74(6)	Aℓ	GIF†	31 Aug 83	0.099 ±0.008	5
6.00(6)	SS	RS2	6 Jun 83	0.097 ±0.011	10
6.77(6)	SS	GIF	31 Aug 83	0.089 ±0.006	5
7.74(6)	Aℓ	RS2	Apr 82	0.125 ±0.002	2
7.74(6)	Aℓ	RS2	Jun 82	0.103 ±0.004	10
7.90(6)	Aℓ	RS2	31 May 83	0.109 ±0.004	5
7.77(6)	SS	RS2	22 Aug 83	0.163 ±0.005	5
1.03(7)	Aℓ	RS2	Apr 82	0.178 ±0.019	2
1.55(7)	Aℓ	RS2	Apr 82	0.236 ±0.008	2
1.56(7)	Aℓ	RS2	Jun 82	0.199 ±0.007	10
1.48(7)	SS	GIF	17 Apr 80	0.243 (±0.008)	1
3.71(7)	SS	GIF	17 Apr 80	0.594 (±0.037)	3
7.42(7)	SS	GIF	17 Apr 80	1.398 (±0.087)	1

*EG&G/EM Santa Barbara Operations source array.
†Sandia Corporation source array.

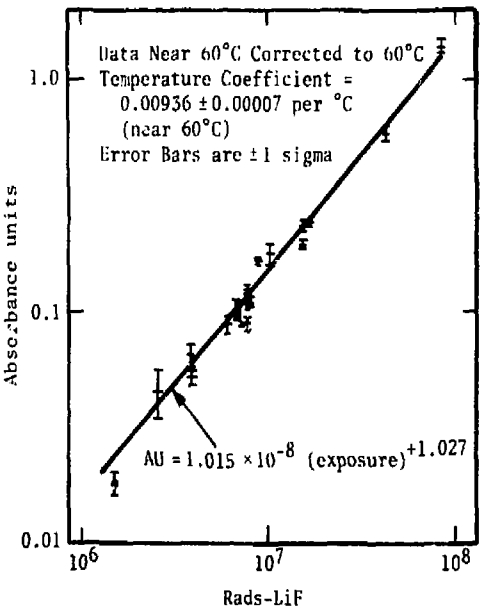

Figure 1. 374-nm peak AU polished LiF, 2-mm thickness

4. REEVALUATION OF 247-nm CALIBRATION DATA

The 247-nm exposure range covers 2×10^3 to 1×10^7 rads-LiF. All previous calibration exposures were originally made at EG&G/EM Santa Barbara Operations, but at various temperatures. In view of the temperature sensitivities found for the other peaks, a new set of exposures was made at 60°C to extend and confirm previous data. Two separate sources were used, both ^{60}Co. Readout was done with both the Beckman 5270 spectrophotometer and the modified IL500 device (see EG&G Report No. EGG 1183-2455).[3] The latter instrument had originally been planned for use as a second measurement tool, but unfortunately the Climax wall exposures were at the upper limit of its capabilities. The data presented here illustrate the wide range of exposures possible with this system and are a consistent set. Similar data were presented in EG&G Report No. EGG 1183-2455, but the present set was derived from a new series of exposures.

No temperature corrections were applied to the data since all of it was taken with a temperature-controlled holder at 60°C. Since all of the Climax data at 0.51 and 0.66 m are within ±5°C of 60°C, an extensive temperature effects study was not undertaken. Very early data (reported in EG&G Report No. EGG 1183-2342, October 1981)[2] at 25°C-30°C irradiation temperature did display a different slope above $\sim 2 \times 10^5$ rads-LiF. The present data are best fit (see discussion below) by a power curve with a slope change near 1×10^5 rads-LiF. It is not clear whether these differences are significant.

The calibration data, presented in Table 2, were obtained in separate sequential exposures using two different ^{60}Co sources at EG&G/EM Santa Barbara Operations. The exposure rate from each source was determined with an NBS traceable ion chamber. Source RS1 is a collimated point source; RS2 is an annular array and was also used for the 374-nm work. The same set of 10 dosimeters was used for all data. There was no bakeout between exposures. The dosimeters were allowed to come to temperature equilibrium in the exposure holder (approximately 10 minutes) before each exposure was started.

Both the Beckman 5270 and the IL500 instrument were used for readout. The IL500 had been modified as described previously to use a high-pressure, mercury vapor light source. The 5270 spectrophotometer was unable to measure densities greater than $\sim$1.5 AU, which corresponds to $\sim 9 \times 10^5$ rads-LiF. The IL500 provided data from $\sim$0.1 AU up to 4.5 AU, where it too lacked good signal to noise ratio. This considerable overlap showed good agreement between the two instruments and reinforced our calibration in AU of the modified IL500.

The Table 2 data, plotted in Figure 2, were fitted with weighted least squares power curves. We extended the lower exposure end as far as could be done to help define the slope below 10^5 rads-LiF. The two curves have the following equations:

$$AU = (1.06 \pm 0.71) \times 10^{-4} \text{ (rads-LiF)}^{0.755 \pm 0.063}$$

Table 2. 247-nm calibration data at 60°C*

Rads-LiF Exposure†	^{60}Co Source	Beckman 5270 AU ± 1 Sigma	IL500 AU ± 1 Sigma
1.64(3)	RS1	0.026 ± 0.004	
3.29(3)	RS1	0.036 ± 0.005	
6.58(3)	RS1	0.066 ± 0.007	
7.67(3)	RS2	0.103 ± 0.006	0.080 ± 0.016
1.53(4)	RS2	0.165 ± 0.018	0.155 ± 0.024
2.95(4)	RS1	0.233 ± 0.025	
3.83(4)	RS2	0.298 ± 0.030	0.280 ± 0.030
7.66(4)	RS2	0.490 ± 0.050	0.500 ± 0.050
1.53(5)	RS2	0.704 ± 0.058	0.780 ± 0.070
3.83(5)	RS2	1.09 ± 0.10	1.14 ± 0.10
7.66(5)	RS2	1.49 ± 0.11	1.55 ± 0.11
1.53(6)	RS2		2.06 ± 0.14
3.83(6)	RS2		3.28 ± 0.14
7.66(6)	RS2		4.41 ± 0.08

*For all exposures, holder material was aluminum; 10 dosimeters per point used for all data.
†1.89(3) means 1.89×10^3, etc.

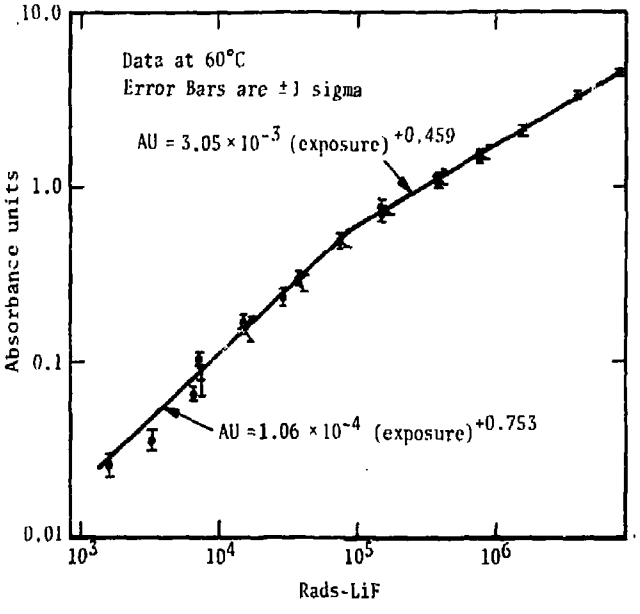

Figure 2. 247-nm peak AU polished LiF, 2-mm thickness

over the exposure range from 2×10^3 to 1×10^5 rads-LiF with a correlation coefficient of 0.989, and

$$AU = (3.05 \pm 0.23) \times 10^{-3} \text{ (rads-LiF)}^{0.459 \pm 0.029}$$

over the exposure range from 1×10^5 to 9×10^6 rads-LiF with a correlation coefficient of 0.9995. The resulting curves are very similar in shape and magnitude to those presented in EG&G Report No. EGG 1183-2455.[3]

The 0.51-m data happen to fall on the upper curve while the 0.66-nm data are all on the lower curve. Fortunately no points are close to the slope change region and hence it was not more thoroughly explored. It should be pointed out that the slope change is not an artifact of the two sources used to cover the exposure range. As shown in Table 2, this occurs at 3×10^4 rads-LiF and there are two overlapping points. Similarly the readout instruments overlap throughout the central region. Thus it seems that curves are on a firm footing, and they were used as shown for data reduction in the next section.

5. CORRECTED CLIMAX DATA

Tables 3, 4, and 5 contain all of the long-term Climax exposure data read out at 247-nm and 374-nm and evaluated with the calibration information in the preceding sections. Data at 443 nm have been omitted since no work was done to unravel the large temperature coefficient previously demonstrated for this peak.

The maximum temperatures used are those provided by W. Patrick (letter dated 27 Feb 1984) and are a consistent set. They differ in some locations from temperature data used previously. A Gaussian shape was used as a convenient tool to interpolate temperature versus axial distance along the fuel center line.

The AU values are those previously reported and are unchanged. The data from the dosimeters removed on 8 Mar 1983 are new.

The fractional fade data were recalculated based upon the most recent temperature information. In light of the temperature sensitivity problems discussed in previous sections the original fade data were reexamined. It is clear that this method of correction for fade is only a first approximation. However, acquisition of a better set of data would be very time-consuming and it doesn't seem justified for the 374-nm data where fade corrections are at worst 5%. The 247-nm data from 0.51 m and 0.66 m have fade corrections of nearly 30%. While these are consistent with previously reported references, they are large nevertheless. Separate columns of estimated exposure before and after fade corrections are provided.

These data have an overall accuracy of approximately ±6% at best. This is made up of ±4% due to errors in transfer of the NBS standard, with the remainder associated with reading errors. The effects of temperature during irradiation have been examined, and the corrections determined probably contribute no more than an additional ±5% for the 374-nm data. The 247-nm data seem to show a smaller temperature coefficient (at least below 10^5 rads-LiF) but it has not been examined in detail. The new 60°C calibration curve at 247-nm has minimized any uncorrected effects of temperature, since the Climax field data are within ±5°C of this temperature. Thus a conservative estimate of temperature-caused errors of the 247-nm data is ±5%, in addition to the radiological associated error of ±6%.

Table 3. Exposures in rads-LiF between April 1980 and 12 Jan 1981*

Hole Number, Dosimeter Location	Vertical Distance From Midplane (m)	Maximum Temp. °C	247 nm				374 nm				
			AU	Raw Exposure†	Fractional Fade	Fade-Corrected Exposure	Raw AU	60°C AU	Raw Exposure†	Fractional Fade	Fade-Corrected Exposure
CEH1	+1.22	67.1					0.380	0.406	2.68(7)	1.03	2.60(7)
(wall)	0	70.4					0.435	0.478	3.15(7)	1.03	3.06(7)
	-1.22	63.2					0.392	0.414	2.74(7)	1.04	2.65(7)
CEH3	+1.83	67.3					0.161	0.172	1.16(7)	1.03	1.13(7)
(wall)	+1.22	73.5					0.434	0.490	3.22(7)	1.02	3.16(7)
	+0.61	76.7					0.444	0.514	3.58(7)	1.01	3.55(7)
	0	76.5					0.491	0.568	3.72(7)	1.01	3.68(7)
	-0.61	72.8					0.483	0.541	3.55(7)	1.02	3.48(7)
	-1.22	66.3					0.540	0.572	3.75(7)	1.04	3.61(7)
	-1.83	57.7					0.201	0.197	1.33(7)	1.05	1.27(7)
CEH3	+1.22	64.8	1.424	6.95(5)*	0.72	9.65(5)	0.011	0.012	8.70(5)	1.04	8.37(5)
(0.51 m)	0	68.1	1.210	4.87(5)	0.70	6.96(5)	--	--	--		--
	-1.22	61.9	1.223	4.99(5)	0.73	6.84(5)	~0.01	~0.01	~7.3 (5)	1.04	~7.0 (5)
CEH3	+1.22	60.4	0.373	5.45(4)	0.73	7.47(4)	--				
(0.66 m)	0	63.9	0.416	6.30(4)	0.72	8.75(4)	--				
	-1.22	59.6	0.457	7.13(4)	0.74	9.64(4)	--				
CEH4‡	+1.22	77.4					0.062		4.31(6)	1.00	4.31(6)
(heater)	0	78.8					0.738		4.80(7)	1.00	4.80(7)
(wall)	-1.22	64.6					>3		--	1.04	--
CEH7	+1.22	69.4					0.400	0.436	2.88(7)	1.03	2.80(7)
(wall)	0	72.2					0.408	0.455	3.00(7)	1.02	2.94(7)
	-1.22	62.7					0.515	0.528	3.47(7)	1.04	3.34(7)
CEH11	+1.22	71.4					0.377	0.418	2.76(7)	1.02	2.71(7)
(wall)	0	77.5					0.395	0.461	3.04(7)	1.00	3.04(7)
	-1.22	70.9					0.354	0.391	2.59(7)	1.02	2.54(7)

*7.49(5) means 7.45×10^5, etc., throughout table.
†Includes 1.063 attenuation correction for dosimeter holder.
‡CEH4 had predoses of 8.5(6), 5.6(7), and 2.9(8).

Table 4. Exposures in rads-LiF between 12 Jan 1981 and 23 Oct 1981*

Hole Number, Dosimeter Location	Vertical Distance From Midplane (m)	Maximum Temp. °C	247 nm				374 nm				
			AU	Raw Exposure†	Fractional Fade	Fade-Corrected Exposure	Raw AU	60°C AU	Raw Exposure†	Fractional Fade	Fade-Corrected Exposure
CEH1 (wall)	+1.22	62.6					0.33	0.34	2.26(7)	1.04	2.17(7)
	0	66.4					0.35	0.37	2.45(7)	1.03	2.38(7)
	-1.22	59.5					0.35	0.35	2.32(7)	1.05	2.21(7)
CEH3 (wall)	+1.22	64.1					0.33	0.34	2.26(7)	1.04	2.17(7)
	+0.61	59.4					0.34	0.34	2.26(7)	1.05	2.15(7)
	0	72.1					0.37	0.41	2.71(7)	1.02	2.66(7)
	-0.61	72.1					0.39	0.44	2.90(7)	1.02	2.84(7)
	-1.22	69.3					0.38	0.41	2.71(7)	1.03	2.63(7)
	-1.83	64.0					0.153	0.159	1.08(7)	1.04	1.04(7)
	-2.44	56.8	0.39	5.78(4)*	0.75	7.71(4)	<0.01	--	--	1.05	--
CEH3 (0.51 m)	+1.22	62.1	1.38	6.49(5)	0.73	8.89(5)	~0.01	~0.01	~7.3 (5)	1.04	~7.0 (5)
	0	65.3	1.29	5.60(5)	0.71	7.89(5)	<0.01	--	--	1.04	--
	-1.22	60.3	1.36	6.28(5)	0.73	8.60(5)	<0.01	--	--	1.04	--
CEH3 (0.66 m)	+1.22	58.5	0.36	5.20(4)	0.74	7.03(4)					
	0	61.7	0.35	5.01(4)	0.73	6.86(4)					
	-1.22	58.3	0.31	4.26(4)	0.74	5.76(4)					
CEH4‡ (heater)	+1.22	72.2					0.021		1.50(6)	1.02	1.47(6)
	0	73.5					0.23		1.54(7)	1.02	1.51(7)
(wall)	-1.22	62.3					>3.0		--	1.04	--
CEH7 (wall)	+1.22	61.7					0.34	0.35	2.32(7)	1.04	2.23(7)
	0	69.1					0.31	0.34	2.26(7)	1.03	2.19(7)
	-1.22	61.8					0.36	0.37	2.45(7)	1.04	2.36(7)
CEH11 (wall)	+1.22	68.3					0.31	0.33	2.19(7)	1.03	2.13(7)
	0	73.9					0.33	0.37	2.45(7)	1.02	2.40(7)
	-1.22	68.7					0.33	0.36	2.39(7)	1.03	2.32(7)

*6.29(4) means 6.29×10^4, etc., throughout table.
†Includes 1.063 attenuation correction for dosimeter holder.
‡CEH4 had predoses of 4.8(6), 1.9(7), and 4.8(8).

Table 5. Exposures in rads-LiF between 23 Oct 1981 and 8 Mar 19[illegible]

Hole Number, Dosimeter Location	Vertical Distance From Midplane (m)	Maximum Temp. °C	247 nm				374 nm				
			AU	Raw Exposure†	Fractional Fade	Fade-Corrected Exposure	Raw AU	60°C AU	Raw Exposure†	Fractional Fade	Fade-Corrected Exposure
CEH1 (wall)	+1.22	56.8					0.414	0.401	2.65(7)	1.05	2.52(7)
	0	59.8					0.465	0.464	3.06(7)	1.05	2.91(7)
	-1.22	55.8					0.465	0.446	2.94(7)	1.05	2.80(7)
CEH3 (wall)	+1.83	57.9					0.197	0.193	1.30(7)	1.05	1.24(7)
	+1.22	62.0					0.456	0.465	3.06(7)	1.04	2.94(7)
	+0.61	64.3					0.504	0.525	3.45(7)	1.04	3.32(7)
	0	64.5					0.525	0.547	3.59(7)	1.04	3.45(7)
	-0.61	62.7					0.543	0.557	3.65(7)	1.04	3.51(7)
	-1.22	59.0					0.525	0.520	3.41(7)	1.05	3.25(7)
	-1.83	53.8					0.215	0.202	1.36(7)	1.05	1.30(7)
CEH3 (0.51 m)	+1.22	57.0	1.20	4.78(5)*	0.75	6.37(5)	0.01	0.01	7.29(5)	1.05	6.94(5)
	0	59.7	1.07	3.73(5)	0.74	5.04(5)	0.006	0.006	4.43(5)	1.05	4.22(5)
	-1.22	56.4	1.16	4.44(5)	0.75	5.92(5)	0.006	0.006	4.43(5)	1.05	4.22(5)
CEH3 (0.66 m)	+1.22	54.2	0.461	7.22(4)	0.76	9.50(4)					
	0	57.3	0.425	6.48(4)	0.75	8.64(4)					
	-1.22	55.0	0.335	4.72(4)	0.76	6.21(4)					
CEH4‡ (heater)	+1.22	65.2					0.042		2.95(6)	1.04	2.84(6)
	0	66.4					0.729		4.75(7)	1.03	4.61(7)
(wall)	-1.22	57.6					>3		--	1.05	--
CEH7 (wall)	+1.22	59.7					0.465	0.464	3.06(7)	1.05	2.91(7)
	0	62.9					0.474	0.487	3.20(7)	1.04	3.08(7)
	-1.22	58.5					0.534	0.526	3.45(7)	1.05	3.29(7)
CEH11 (wall)	+1.22	61.7					0.450	0.457	3.01(7)	1.04	2.89(7)
	0	66.5					0.453	0.481	3.17(7)	1.03	3.08(7)
	-1.22	63.3					0.450	0.464	3.06(7)	1.04	2.94(7)

*5.16(5) means 5.16×10^5, etc., throughout table.
†Includes 1.063 attenuation correction for dosimeter holder.
‡CEH4 had predoses of 3.9(6), 2.8(7), and 9.6(7).

6. DISCUSSION

The data presented appear to have solved the various questions raised in the preceding two reports, i.e., there is a temperature effect on both the 247-nm and 374-nm peaks. For purposes of data handling, this temperature effect can be resolved into 1) a change in sensitivity versus temperature during irradiation, and 2) a fading effect similar to that seen in other dosimetric systems such as TLD's that affects the stability of the readout data. It should be pointed out however that this separation of effects must be reevaluated after a better understanding of the kinetics of fading is available.

The sensitivity change versus irradiation temperature is nearly 1% per °C at a nominal 60°C for the 374-nm peak. A reasonable amount of data was collected to document this sensitivity and it has allowed corrections to be made to all Climax data at this wavelength. The 247-nm peak also has a sensitivity change versus irradiation temperature, but at present this is less well documented. Below 1×10^5 rads-LiF we found only a very small change between 25°C and 60°C, less than 5%. Above 1×10^5 rads-LiF an apparently larger temperature effect is present, but was not directly measured. Instead, a new calibration curve was made at a temperature of 60°C that is within 5°C of all field data. This should permit evaluations to be made with little error due to temperature.

The fade effects reported in EG&G Report No. EGG 1183-2432 (October 1981)[2] were used unchanged for the current reevaluation except where better temperature data required a change. The magnitudes of the fade corrections are small for the 374-nm peak and considerably larger for the 247-nm peak. This is consistent with literature references, but does imply a larger error in the 247-nm peak data due to the relatively simple way in which the fade corrections were made.

In conclusion it is believed that the present set of data contain the fewest uncertainties of all data taken thus far. The temperature effects on sensitivity during irradiation are new and have not been documented previously. They were determined here only near 60°C with enough accuracy and precision for the task at hand, but it appears that similar effects occur at other temperatures. Corrections were made to the field data for this temperature effect as well as for fade of the optical density created by irradiation. The wall material of the dosimeter holders both in the field and in laboratory calibrations were accounted for. The most recent field temperatures were incorporated into the data and corrections made where necessary. And lastly, several source recalibrations were done with NBS traceable three-terminal ion chambers. These sources were then used in the LiF dosimeter calibration.

REFERENCES

1. Quam, W., D. Sever, and T. DeVore, "Climax Spent Fuel Dosimetry – Progress to 7 February 1980," EG&G Report No. EGG 1183-2432 (February 1980).

2. Quam, W. and T. DeVore, "Climax Spent Fuel Dosimetry – Progress Report September 1980 to September 1981," EG&G Report No. EGG 1183-2432 (October 1981).

3. Quam, W. and T. DeVore, "Climax Spent Fuel Dosimetry – Progress Report September 1981 – September 1982," EG&G Report No. EGG 1183-2455 (August 1982).

4. Quam, W. and T. DeVore, "Climax Spent Fuel Dosimetry, Short Term Exposure, 8 March 1983," EG&G Report No. EGG 10282-2041 (June 1984).

APPENDIX: CALIBRATION OF LiF CHIPS FOR OPTICAL ABSORPTION READOUT

A1. INTRODUCTION

The calculation of absorbed dose in various media when exposed to a gamma ray fluence is usually assisted by placement of an imaginary non-absorbing and non-perturbing small cavity in the medium. The calculated energy deposition in this cavity is then proportional to the kerma in the cavity wall, since the postulated conditions result in charged particle equilibrium in the cavity vicinity. Calculation of the energy deposited in this cavity is relatively simple and depends upon electron stopping powers of the cavity material (since the cavity is small compared to the electron range) and mass energy absorption coefficients of the wall material. Detailed descriptions of these methods are given in NBS Handbooks 78 and 79.[A1,A2]

In the case at hand however, the "cavity" used is a LiF chip which is not a non-absorbing detector in the usual Bragg-Gray sense treated in the NBS handbooks. The LiF chips used were approximately $0.5 \times 0.2 \times 0.2$ cm. The maximum electron range in LiF from electrons produced by 1.25-MeV gammas is approximately 420 mg/cm^2 or 0.16 cm. Hence the chip severely attenuates any electrons produced in the wall of its holder or "medium." The attenuation is worse for a 0.5-MeV gamma exposure, which results in a maximum electron range of 0.04 cm in LiF. The chip is thus not a Bragg-Gray cavity/medium situation, but more nearly one treated by Burlin.[A3]

Burlin's cavity theory enables calculation of the ratio, f, of the average dose in the cavity $\bar{D}_c$ (i.e., the LiF chip) to the wall kerma, assuming the incident gammas are not attenuated significantly in the wall or cavity. This was given by Burlin as

$$f = \frac{\bar{D}_c}{D_{med}} = d\left(\overline{\frac{(S/\rho)_c}{(S/\rho)_{med}}}\right) + (1-d)\left(\frac{\left(\mu_{en}/\rho\right)_c}{\left(\mu_{en}/\rho\right)_{med}}\right) \qquad (A1)$$

where Burlin assumed $K_{med} = D_{med}$. This latter assumption is true only where charged particle equilibrium exists. D_{med} is not the dose in the cavity wall because the absorbing cavity perturbs the charged particle equilibrium there. It should be interpreted as the dose in the medium at least one electron range away from the cavity.

The first term in Eq. (A1) is the mean value of the mass collision stopping power ratios averaged over the electron spectrum in the cavity. The second term is the ratio of mass energy absorption coefficients for the gamma

rays near the cavity. The dimensionless weighting factor d depends upon the absorption characteristics of the cavity (i.e., chip) for the electrons entering the cavity. When d = 0, the contribution of wall electrons to $\bar{D}_c$ is negligible. An example of this is a cavity large compared to the electron range. This is nearly the case for the LiF chips irradiated with 0.50-MeV gammas and is an adequate approximation for 1.25-MeV gammas. Ogunleye, Attix, and Paliwal[A4] recently examined this theory experimentally using LiF TLD's in a variety of holder materials from LiF to lead. Reasonable agreement (1% to 3%) between theory and experiment was found for polystyrene, aluminum, and copper holders. F. H. Attix[A5] suggested use of d = 0 for the present case based on his experience with Burlin cavity theory. This implies that all the dose deposited in the LiF chips is due to electrons generated within the chip by the incident gamma rays. Presumably the incident electrons from the wall of the holder are balanced by an exiting fluence of electrons from the chip.

A2. CALIBRATION EXPOSURE

The LiF chips were irradiated in aluminum and stainless steel holders with ^{60}Co gamma rays. The gamma exposure was measured with an NBS traceable ion chamber, resulting in R_{cal} roentgens.

The rads-LiF will then be (for the aluminum holder):

$$\text{rads-LiF} = \left(R_{cal}\right)(0.877)\,\frac{\mu_{en}^{LiF}}{\mu_{en}^{air}}\,e^{-\mu_{A\ell}\,A_{A\ell}} \qquad \text{(A2)}$$

where the (0.877) (R_{cal}) is the exposure in rads-air, and the various absorption coefficients[A6] are to be evaluated at 1.25 MeV. The aluminum holder thickness was 0.229 cm. Entering the numbers we have:

$$\text{rads-LiF} = \left(R_{cal}\right)(0.877)\,\frac{0.0246}{0.0267}\,e^{-(0.150)(0.229)} = 0.774\,R_{cal}$$

For the stainless steel holder we have:

$$\text{rads-LiF} = \left(R_{cal}\right)(0.877)\,\frac{0.0246}{0.0267}\,e^{-(0.427)(0.0914)} = 0.777\,R_{cal}$$

These constants were used to calculate the rads-LiF for each exposure from the rads-air measured with an NBS traceable ion chamber. A calibration curve was constructed for each of the two peaks of interest, 247 nm and 374 nm, by measuring the absorbance units, AU, of chips exposed to a wide range of doses.

These data or a fitted line on the calibration curve can be used to determine a relationship between rads-LiF and AU that will allow AU from a field exposure to be converted to rads-LiF. Thus we may calculate:

$$\left(\frac{\text{rads-LiF}}{\text{AU}}\right)_{\text{cal}}$$

at several exposure levels and use this information to reduce the field data.

A3. FIELD EXPOSURE

The chips were exposed in the field in stainless steel holders (identical to those used in some calibration irradiations). These holders had 0.0914-cm-thick walls at the location of the dosimeters. The exposure at the exterior of this holder, but within the permanently installed dosimeter tubes, is:

$$(\text{rads-LiF})_{\text{field}} = \text{AU}_{\text{field}} \left(\frac{\text{rads-LiF}}{\text{AU}}\right)_{\text{cal}} e^{+\mu_{SS} X_{SS}}$$

where μ_{SS} is evaluated at the effective energy of 0.5 MeV[A7] and $X_{SS} = 0.0914$ cm. This evaluates to:

$$(\text{rads-LiF})_{\text{field}} = \text{AU}_{\text{field}} \left(\frac{\text{rads-LiF}}{\text{AU}}\right)_{\text{cal}} (1.063) \qquad \text{(A3)}$$

A4. REFERENCES

A1. NBS Handbook 78, Report of the International Commission on Radiological Units and Measurements (ICRU) (1959).

A2. NBS Handbook 79, Stopping Powers for Use with Cavity Chambers (also issued as NCRP 27) (1961).

A3. Burlin, T. E., *Br. J. Radiol., Vol. 39*, p 727 (1966).

A4. Ogunleye, O. T., F. H. Attix, and B. R. Paliwal, *Phys. Med. Biol., Vol. 25*, pp 203-213 (1980).

A5. F. H. Attix, personal communication.

A6. NSRDS-NBS29, Photon Cross Sections, Attenuation Coefficients, and Energy Absorption Coefficients from 10 keV to 100 GeV (1969).

A7. R. Van Konynenburg, personal communication.

DISTRIBUTION

USDOE, Nevada Operations Office
Las Vegas, Nevada

M. P. Kunich
J. Newlin
G. Plummer
M. Schramm
D. L. Vieth

USDOE, Technical Information
Center, Oak Ridge, Tennessee

W. D. Matheny (2)

USDOE, Office of Waste Isolation,
Washington, D.C.

C. R. Cooley
M. W. Frei
R. Stein

USDOE, Office of Geologic Repository
Deployment, Washington, D.C.

W. Bennett

USDOE, Columbus Program Office,
Columbus, Ohio

J. O. Neff

USDOE, Crystalline Rock Project
Office, Argonne, Illinois

N. Bulut
S. A. Mann

USGS, Denver, Colorado

W. Dudley

Battelle, Columbus, Ohio

S. J. Basham
W. Carbiener
S. C. Matthews
R. Robinson
W. Ubbes

Battelle Pacific Northwest Laboratory,
Richland, Washington

D. J. Bradley
B. Johnson

Brookhaven National Laboratory,
Upton, New York

P. W. Levy

E. R. Johnson Associates, Inc.,
Reston, Washington

J. A. Carr

Hanford Engineering Development,
Richland, Washington

R. E. Einziger

Lawrence Livermore National Laboratory,
Livermore, California

L. Ballou
R. Carlson
W. Durham
D. Montan
W. Patrick
V. Oversby
R. Ryerson
R. Van Konynenburg
T. Wilcox
NWM Library (10)

Los Alamos National Laboratory,
Los Alamos, New Mexico

D. Oakley

Rockwell Hanford Operations,
Richland, Washington

K. Kim

Sandia National Laboratory,
Albuquerque, New Mexico

J. K. Johnstone
T. Hunter
L. W. Scully
L. D. Tyler

Science Applications, Inc.
Las Vegas, Nevada

M. Spaeth

Westinghouse Electric Corporation,
Mercury, Nevada

A. R. Hakl

Westinghouse Electric Corporation,
Pittsburgh, Pennsylvania

J. B. Wright

EG&G/EM, Las Vegas Operations,
Las Vegas, Nevada

T. O. Edward
Library

EG&G/EM, Santa Barbara Operations,
Goleta, California

T. DeVore
W. Quam (10)
Publications (9)